ACS Catalysis

pubs.acs.org/acscatalysis
Research Article

Flexible Biguanide Mono- and Bimetallic Zinc Complexes for the Ring-Opening (Co)polymerization of Lactides

Benjamin Théron,[§] Lukáš Vlk,[§] Tomáš Chlupatý,* Marie-José Penouilh, Eliška Procházková, Raluca Malacea-Kabbara, Pierre Le Gendre,* and Aleš Růžička*

Cite This: *ACS Catal.* 2025, 15, 9117−9129
Read Online

ACCESS | Metrics & More | Article Recommendations | Supporting Information

ABSTRACT: One of the most urgent social demands on polymer chemistry is the design of an inexpensive, efficient, robust, and nontoxic catalyst for the preparation of biodegradable polymers with good control of its properties. The nonsymmetric ditopic doubly deprotonable biguanide proligand (substituted 4,6-dimethoxypyrimidin-2-yl-guanidine − **1**) with dynamic behavior forms monometallic as well as bimetallic complexes when reacted with one or two equivalents of Et_2Zn or $Zn[N(SiMe_3)_2]_2$. In monometallic complexes **2** and **4**, zinc atoms primarily occupy a position within the six-membered ring. In the bimetallic complexes **3** and **5**, the adjacent ethylzinc and zinc amide moieties are coordinated in a bidentate fashion by the guanidinate-like part of the ligand. The ethylzinc complexes **2** and **3** are inactive in the ring-opening polymerization (ROP) of *rac*-lactide, whereas the performance of the zinc amides **4** and **5** activated by ^{i}PrOH is among the highest observed. In complex **5**, the positions of the two zinc ions can be interchanged, which could explain the ability of this "nonsymmetrical" bimetallic complex to promote the ROP of lactide (LA) at both Zn sites to form polylactide (PLA) chains with a unimodal molecular-weight distribution. One-pot preparation of various di- or oligoblock copolymers is possible by the sequential living copolymerization of *β*-butyrolactone and *L*-, *D*- or *rac*-lactides, leading to the precise control of its microstructure.

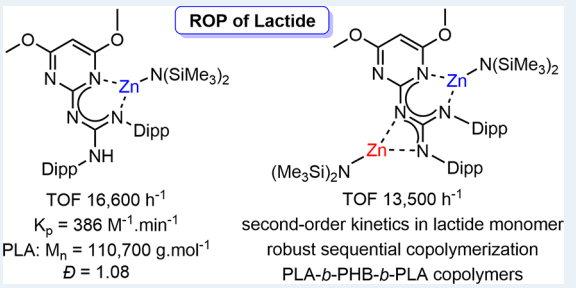

KEYWORDS: *biguanide, zinc, ROP, copolymer, immortal polymerization*

INTRODUCTION

After a hundred years of continuous development, polymeric materials based on repeating units of main-group elements have found widespread practical application in both everyday life and industry. Conventional (i.e., petroleum-based non-biodegradable) plastics have transformed our society and are used in all aspects of our daily lives. However, their impact on the environment is considerable and is no longer tolerable. Polylactide (PLA) is the most promising biobased and biodegradable alternative to petrochemical plastics.[1] It is now being successfully employed in various fields such as 3D printing, medical applications, food packaging, disposable tableware, textiles, agriculture and automotive.[2] A downside to this development is that the industrial production of PLA is mainly attached to the ring-opening polymerization (ROP) of lactide in the presence of tin octoate, whose impact on the environment remains questionable. Great efforts have been devoted to the development of tin-free catalysts. As metal complexes and organometallic species often suffer from the presence of toxic heavy or expensive noble metals and high specificity for a desired reaction or process, one possibility is the application of post-transition metals, specifically zinc and its complexes, which have already shown their potential in many organic transformations or as cheap, environmentally benign, and sustainable alternatives to conventional transition-metal catalysts. Zinc catalysts provide some of the best performance in the ROP of lactides, notably, in terms of activity. The pioneering works of Coates have shown that *β*-diketiminate (BDI) ligands associated with Zn(II) lead to highly efficient systems (Figure 1).[3] More recently, Robinson has described exceptional activity at room temperature for the ROP of LA (TOF_{max} = 13,950 h^{-1}) using Zn complexes supported by a nonsymmetrical version of these BDI ligands (*N*-Aryl/*N*-alkyl).[4]

Remarkably, the highest TOF (60,000 h^{-1}), reported by Williams,[5] has been reached by a dizinc catalyst also coordinated by a "BDI-like" ligand, which can be classified as ditopic as well. Coles[6] and Pellecchia[7] have demonstrated that highly *π*-electrons conjugated guanidinate ligands associated with zinc are also pertinent to the lactide ROP reaction. Recently, epoxide-promoted polymerization of lactides medi-

Received: March 3, 2025
Revised: April 30, 2025
Accepted: April 30, 2025
Published: May 14, 2025

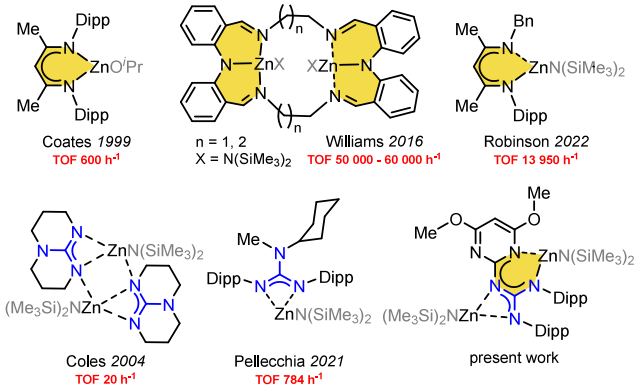

Figure 1. Most active BDI (ring highlighted in gold), BDI-like, and guanidinate (in blue) zinc complexes in lactide ROP.

ated by the low loading of the zinc-guanidine complex has been tested under industrial conditions.[8] In addition, during the completion of this work, Robinson reported on stereoblock polyesters via irreversible chain-transfer ring-opening polymerization using a combination of the previously reported highly active lactide polymerization process promoted by zinc BDI species[4] and the yttrium phenoxide co-initiated polymerization of β-butyro- or β-valerolactone, yielding stereoblock atactic-syndiotactic polyhydroxyalkanoates with good control of the composition, molecular weight and mechanical properties.[9] As summarized in the excellent review on strategies for preparation of stereoblock copolymers by Mehrkhodavandi,[10] the most efficient catalytic systems are based on versatile indium[11−14] and magnesium[15,16] complexes or tin octoate.[17] It is worth noting that zinc-based initiators also allowed excellent access to various oligo-block polyesters and carbonates. Pellecchia[18] and Phomphrai[19,20] made their lactide homo- and copolymeric materials thanks to pyridylamido or phenoxyamido zinc initiators.

During the last 15 years, reports on block polyhydroxybutyrate-containing copolymers, which exhibit interesting material properties, were rather scarce. Rieger[21] used zinc β-diketiminate complexes as initiators of terpolymerization of β-butyrolactone, oxiranes and CO_2. Aluminum-based salen,[22] phenoxyimine[23,24] and phenolate[25] catalysts were also able to promote β-butyrolactone and lactide copolymerization with narrow polydispersities of the formed chains. Indium complexes from the family of multitalented indium salan chlorides or alcoholates[11−14] were later shown to be active with low catalyst loadings[13] or under air atmosphere,[14] albeit with reaction times of 16 h. Other groups used yttrium,[22,26] hafnium[27] and copper[28] metals bearing mostly *N*- and *O*-donor ligands. For the first time, a triblock PLA-*b*-PHB-*b*-PLA was obtained in 2013[11] through sequential addition of the monomers.

Based on these literature facts, we hypothesized that the biguanide derivative **1** (Figures 1 and 2), mimicking both BDI and guanidinate moieties, with highly conjugated π-electron density and structural versatility, could be a suitable ligand to chelate one or two Zn atoms in a variable bonding fashion and (co)-initiate the ROP of lactides efficiently.

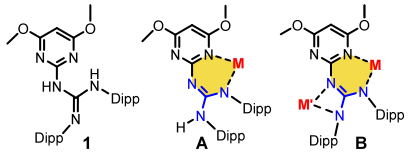

Figure 2. Possible monometallic **A** and bimetallic **B** complexes (among others) obtained from biguanide proligand **1**.

RESULTS AND DISCUSSION

Synthesis and Characterization of Zinc Complexes. The biguanide proligand **1** was prepared according to our previous paper from extremely cheap chemicals by one-pot high-yield synthesis (see SI).[29] Thanks to the connection of a pyrimidine-2-amine moiety and a guanidine fragment, the structure of **1** resembles a part of such macrocyclic ligands as porphyrines, phthalocyanines and other biologically important species (guanine derivatives), but, more interestingly, also a substituted biguanide, which demonstrated biological activity and medicinal applications as well.[30−33] The structural versatility of highly π-electron conjugated **1** arises from the presence of three types of nitrogen atoms − two pyrimidine nitrogens, two secondary amines and one secondary imine − interconnected via two central carbon atoms (abbreviated as Ar_q^{Gua} and Ar_q^{Prm}) of the planar N_5C_2 skeleton. In **1**, this arrangement leads to the coexistence of different isomers and tautomers in equilibrium (Figure 3). This equilibrium in solution is solvent- and temperature-dependent and can be easily monitored by NMR spectroscopy. In both nonpolar (C_6D_6) and polar (THF-d_8) solvents, two sets of signals (the ratios of 90:10 in THF-d_8 and 95:5 in C_6D_6 at room temperature) were detected, indicating the presence of two different species. DFT calculations uncovered four possible forms. While two tautomers are energetically close to each other (**1A** and **1B**; less than 1 kcal/mol), another two possible forms with ΔG values of 4.3 and 7.8 kcal/mol are higher than that of the tautomer **1A**, indicating less than 1% population in the equilibrium (details in SI, page S10). For further investigation of these tautomeric equilibria, the experimental ^{13}C chemical shifts were correlated to the calculated chemical shielding constants. The correlations (Figure S7 in SI) indicated that the major form in THF was the enamine tautomer **1A**, while the minor form was identified as the imine tautomer **1B**. The tautomer **1A** was also found in solid state by scXRD techniques (Figure S9 in SI).

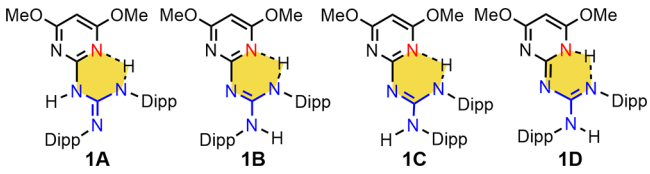

Figure 3. Possible tautomers/isomers of proligand **1**.

Generally, such a nonsymmetrical biguanide structure can be seen as a potentially doubly deprotonable proligand with the possibility of "aza-β-diketiminate" or guanidinate-chelate-ring formation. Surprisingly enough, structurally close but symmetric bis-guanidinate zinc hydride and ditopic conjugated bis-guanidine aluminum and lithium complexes able to chelate two metal atoms have very recently been used for the catalytic reduction of heteroallenes or carbonyl groups.[34−37]

To confirm or disprove our hypothesis, we prepared mono/homobimetallic zinc biguanide complexes **2**−**5** in excellent isolated yields of over 80% (Scheme 1). Particularly, the reaction of an equimolar amount of diethylzinc or zinc

https://doi.org/10.1021/acscatal.5c01335
ACS Catal. 2025, 15, 9117−9129

bis(hexamethyldisilazide) with proligand **1** has afforded isostructural complexes **2** and **4**.

Scheme 1. Synthesis of the Mono-/Homobimetallic Zinc Biguanide Complexes 2−5[a]

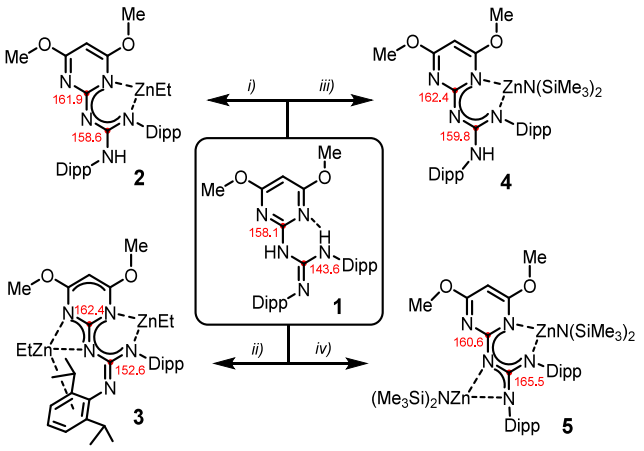

[a] *i*) Et_2Zn, hexane, −80 °C to RT, 24 h; *ii*) 2 Et_2Zn, Et_2O, −80 °C to RT, 7 h; *iii*) $Zn[N(SiMe_3)_2]_2$, Et_2O, −80 °C to RT, 24 h; *iv*) 2 $Zn[N(SiMe_3)_2]_2$, Et_2O, − 80 °C to RT, 7 days. Significant ^{13}C NMR chemical shifts (δ of Ar_q^{Prm} and Ar_q^{Gua}) are highlighted in red and marked with red dots − for **5**, the values recorded at 373 K are presented.

Only one resonance for a hydrogen atom belonging to the NH group at 5.50 and 5.62 ppm in C_6D_6 has been detected in the ^1H NMR spectra of **2** and **4**, respectively (Figures S63 and S79 in SI). These hydrogen atoms are undoubtedly connected to the nitrogen atoms of the Dipp groups as corroborated by 2D NMR techniques (^1H,^{13}C-HMBC, Figures S66−S67 and S82−S83 in SI). The chemical-shift values are up to 4 ppm upfield-shifted when compared to the same parameter found for starting **1**. An obvious explanation arose from the fact that the NH group is not connected by a hydrogen bridge to another part of the molecule. This arrangement is only possible when the zinc atom is coordinated to the six-membered ring. Unlike in **1**, there is no hydrogen atom on the central nitrogen (or N3 according to the crystallographic numbering − Figure 4) in **2** and **4**, with this deprotonated nitrogen being part of a highly conjugated π-electron system. The observed phenomenon is also reflected in the remarkable downfield shift ($\Delta\delta$ = 15 ppm) of the Ar_q^{Gua} carbon atom in the ^{13}C NMR spectra of both **2** and **4** complexes measured in C_6D_6. On the other hand, all Ar_q^{Prm} carbon atoms resonate at a similar value (∼162 ppm) (Scheme 1).

The solid-state behavior of the isostructural mononuclear complexes **2** and **4** shows that the zinc atoms are chelated by the N1 and N5 atoms of both pyrimidine and guanidine domains (Figure 4), thus forming six-membered triazazincacycles, which are reminiscent of the zinc β-diketiminate complexes,[38−41] phthalocyanines,[42] or guanidinates and biguanides.[37,43] In both complexes, the interatomic distances are almost the same. Both N2 atoms, bearing acidic hydrogens,

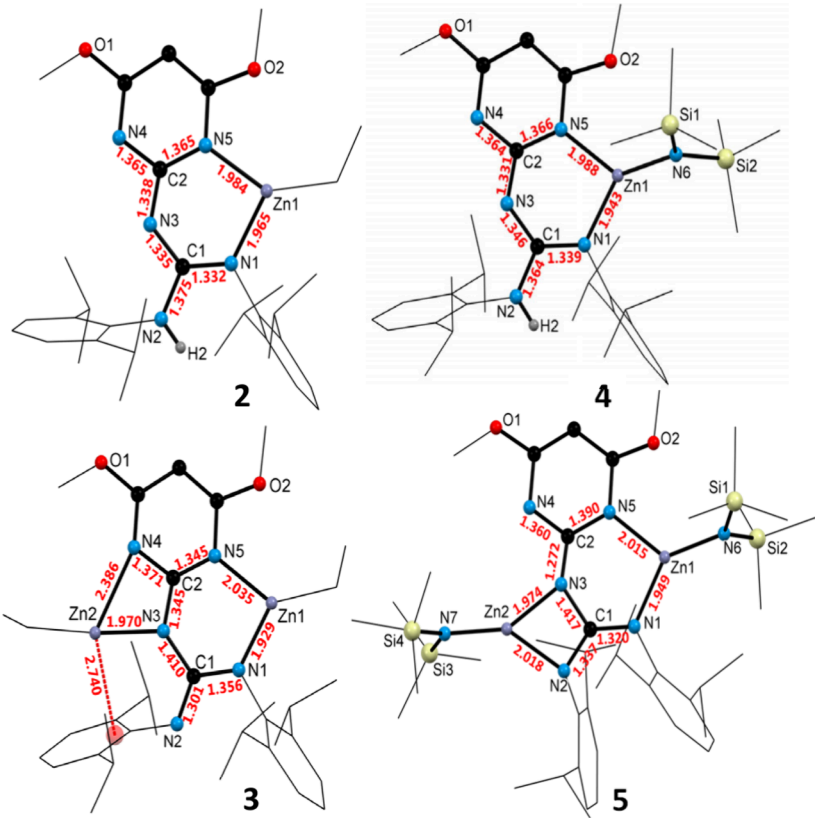

Figure 4. Molecular structures of **2**, **3**, **4** and **5**. Isopropyl, phenyl, ethyl and methyl groups are shown as wireframes for clarity. Selected bond lengths (Å) and angles (°) (in red, without standard deviations) for **2**: C2−N3−C1 126.93(16), N1−C1−N2 118.97(16); for **3**: C2−N3−C1 126.91(10), N1−C1−N2 118.56(9); for **4**: C2−N3−C1 127.7(3), N1−C1−N2 117.5(3); for **5**: C2−N3−C1 132.0(8), N1−C1−N2 131.0(9). The full list of data is given in the SI (Figure S25).

https://doi.org/10.1021/acscatal.5c01335
ACS Catal. 2025, 15, 9117−9129

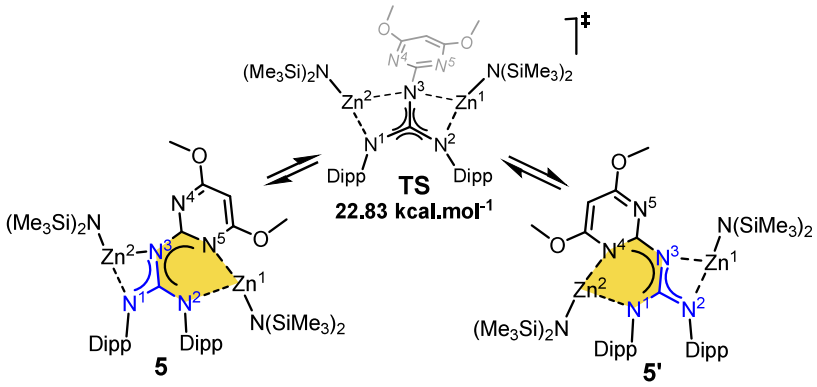

Figure 5. Simplified isomerization pathway of **5** leading to chemically identical species. Only lower energy TS is shown. A more detailed view is given in the SI (Scheme S2).

Table 1. ROP of *rac*-Lactide Mediated by the Biguanide−Zn Complexes 4 and 5 − Selected Experiments[a,b]

Entry	Cat.	[*rac*-LA]:[cat]$_0$:[^{i}PrOH]	time [min]	conv.[c] [%]	$M_{n,\,theo}$[d] [g mol^{-1}]	$M_{n,\,exp}$[f] [g mol^{-1}]	$Đ$[f]	P_r[g]	TOF [h^{-1}]
1	**4**	100:1:0	2 h	61	8,800[e]	188,000	1.11	n.d.	30
2	**5**	100:1:0	2 h	32	2,300[e]	54,100	1.66	n.d.	8
3	**4**	100:1:1	1	98	14,100	13,400	1.07	0.63	5,880
4	**5**	100:0.5:1	1	96	13,800	18,700	1.13	n.d.	5,760
5	**5**	100:1:1	1	80	11,500	15,800	1.24	n.d.	2,400
6	**5**	500:0.5:1	15	86	62,000	69,500	1.38	0.72	1,720
7	**4**	500:1:1	5	98	70,600	57,400	1.21	0.64	5,880
8	**4**	1,000:1:1	5	94	135,000	116,200	1.08	n.d.	11,280
9	**4**	1,000:1:1	3	83	119,600	110,700	1.08	0.65	16,600
10	**5**	1,000:0.5:1	3	43	62,000	60,000	1.40	n.d.	8,600
11	**4**	5,000:1:10	30	88	63,400	55,900	1.04	n.d.	8,800
12	**5**	5,000:0.5:10	20	90	64,900	67,100	1.04	n.d.	13,500

[a]All reactions have been at least duplicated. All the data can be found in SI − Table S2; polymerization conditions: [*rac*-LA]$_0$ = 1.5 M, CH_2Cl_2, 25 °C. [b]Reactions performed with a batch of recrystallized and sublimed LA. [c]Monomer conversion. [d]Calculated using $M_{n,\,theo}$ = [*rac*-LA]$_0$/[^{i}PrOH]$_0$ × M_{LA} × conversion. [e]Calculated using $M_{n,\,theo}$ = [*rac*-LA]$_0$/[Zn]$_0$ × M_{LA} × conversion. [f]Measured by GPC in THF on the crude reaction mixture without precipitation of the polymer (45 °C) using PS standards and corrected by applying the appropriate correction factor (0.58). [g]Determined from the methine region of the HD ^{1}H NMR spectrum.

are a part of a highly π-electrons conjugated planar system, as documented by shortening of C1−N2, compared to a standard C−N distance (Figure 4). The only significant difference in the molecular structures of **2** and **4** is caused by the more sterically demanding disilazide ligand in **4**, which displaces the zinc atom from the plane of the ligand by 0.588 Å.

The same synthetic approach (in Et_2O, −80 °C), in the molar ratio of 1:2, has also been used for the preparation of the homobimetallic zinc biguanides **3** and **5**. In the case of the synthesis of **3**, the reaction procedure is complex, and after the addition of diethylzinc, the reaction time must be limited to 7 h only. When the product is kept in solution for a longer time, the subsequent decomposition of **3** to **2** (and some unidentified ethylzinc moieties) is observed. In order to maximize the yield, different reaction times and stoichiometries have been investigated (for more details, see SI, Figures S14−S26).

The structure of both complexes **3** and **5** was determined by NMR spectroscopy, where the spectral pattern of **3** was similar to that shown in **2** and **4**. However, complex **5** behaved differently, as indicated by the significant NMR-signal broadening. In order to investigate the fluxional behavior of **5**, variable-temperature NMR measurements were performed. Although distinct sets of the signals of peripheral methyl and methine groups (203 K in Tol-d_8; for VT NMR measurements, see SI, Figures S23−S24) were recorded, the spectra exhibit only one set of signals for the biguanide carbon atoms of the core of the compound. In particular, for Ar_q^{Gua}/Ar_q^{Prm}, the resonances were found at 164.9/159.3 ppm (compare with 165.5/160.6 ppm, recorded at 373 K, and with 152.6/162.4 ppm for **3**; see Scheme 1). This indicates that in **5**, the guanidinato group is more involved in the coordination of the second zinc atom than the pyrimidine group. In the ^{1}H NMR spectra, the hydrogen atom located on the top of the pyrimidine part of complex **5** (5.1 ppm at 295 K in C_6D_6) is similarly downfield-shifted to monometallic **2**, **4** and bimetallic **3**, but different by $\Delta\delta$ 0.4 ppm from the value found for the proligand **1**.

The solid-state structure of **3** shows the Zn1 atom chelated in the six-membered ring with a planar arrangement and Zn1−N5 distances that are only about 0.05 Å longer than in **2** (Figure 4). The Zn2 atom is bound anisobidentately to the guanidinate group (Zn2−N3 = 1.9699(17) and Zn2−N4 = 2.3864(18) Å) with the N3−Zn2−N4 angle of 60.69(6)°. The adjacent contact of Zn2 to the neighboring phenyl ring via η^3-fashion (2.740 Å) brings the zinc out of the planar environment of the ligand by 0.269 Å. It seems, that this contact has a bit repulsive character as the C1−N2−C20 and C1−N3−Zn2 angles are slightly wider than 120°. The second compound, dinuclear complex **5**, bearing one disilazide group on each zinc atom, has the ligand core and both zinc atoms nearly in plane. The second change is the inversion at the N2

https://doi.org/10.1021/acscatal.5c01335
ACS Catal. 2025, 15, 9117−9129

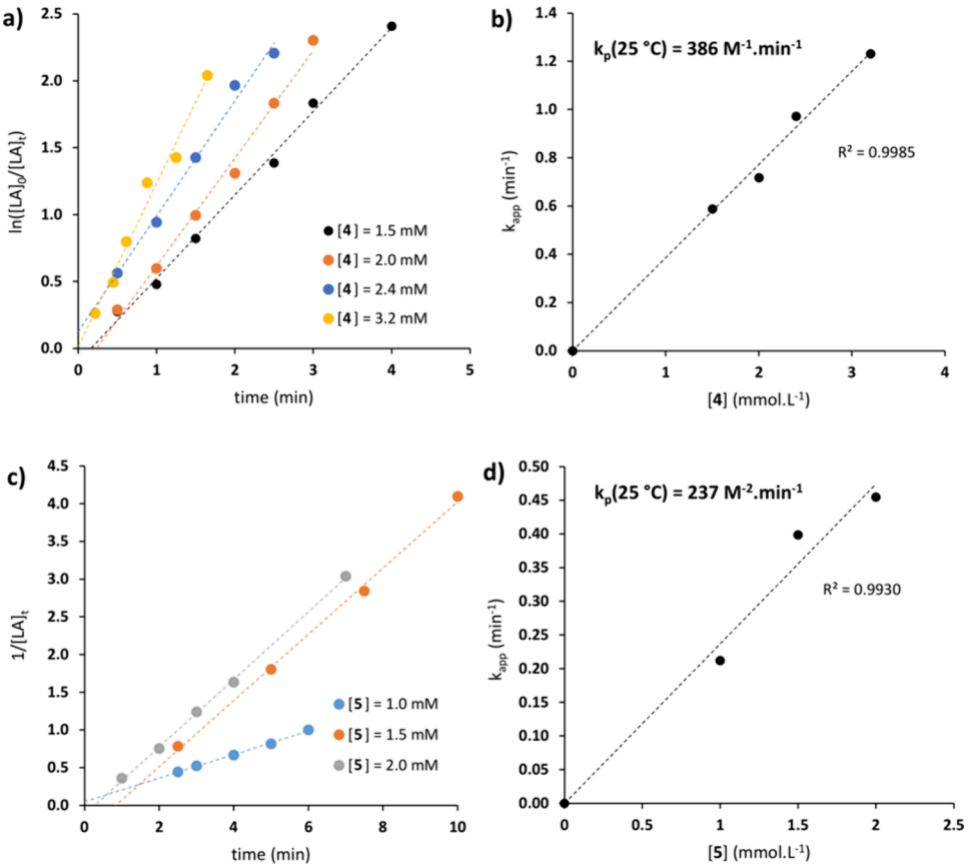

Figure 6. a) A first-order semilogarithmic plot for the polymerization of *rac*-LA at 25 °C in CH_2Cl_2 using **4** at different concentrations with ^{i}PrOH as a co-initiator. b) A plot of k_{app} vs $[\mathbf{4}]_0$. c) A second-order plot for the polymerization of *rac*-LA at 25 °C in CH_2Cl_2 using **5** at different concentrations with ^{i}PrOH as a co-initiator. d) A plot of k_{app} vs $[\mathbf{5}]_0$.

atom, which enabled the isobidentate coordination of the Zn2 atom to the guanidinate moiety by N2 and N3 atoms (1.974(8) and 2.018(8) Å, angle 66.6(5)) (see SI — Figure S25).

To explain the dynamic behavior of **5** in solution, a pendulum-like exchange of the positions of the Zn1 and Zn2 atoms was proposed (Figure 5). This "pendulum" mechanism assumes an inversion at the imino nitrogen N3 as well as the decoordination/recoordination of Zn1 from N5 to N3 and of Zn2 from N3 to N4. The inversion on both methoxy groups should be taken into the account as well. As shown by the solid-state structure of the complex **5**, the unique placement of the two Dipp groups at the base of the ligand unlocks the system and enables this movement. For this sequence of structural changes, we have found a transition state (Figure 5, mol and gif files in SI) whose energy exceeds that of the optimized structure of **5** by 22.83 kcal/mol.

ROP Catalysis. All the monometallic and bimetallic zinc complexes prepared were investigated as catalysts for the ROP of *rac*-LA (reduced in Table 1 and full data in Table S2). The complexes **2** and **3** showed no activity after 2 h at 25 °C in CH_2Cl_2, even in the presence of one equivalent of ^{i}PrOH as a co-initiator. The bis(trimethylsilylamido) complexes **4** and **5** exhibited modest activities, reaching monomer conversion of 61% and 32% in 2 h at 25 °C without ^{i}PrOH (Table 1, entries 1 and 2). Remarkably, the GPC analysis of the PLA chains thus formed showed much higher average molecular weights than the theoretical M_n values calculated on the basis of LA conversion and LA:Cat. ratio. These results suggest a slower initiation than propagation. Unlike in the complexes **2** and **3**, the use of ^{i}PrOH as a co-initiator in the complexes **4** and **5** greatly improved their performance. In the presence of one eq. of alcohol per Zn metal center, both complexes initiated the ROP of 100 eq. of *rac*-LA with almost complete conversion in 1 min and led to slightly heterotactic PLA with narrow dispersity and good agreement between theoretical and experimental M_n values, albeit with slightly higher molar mass than expected in the case of **5** (Table 1, entries 3 and 4). It is noteworthy that an increase in the **5**:^{i}PrOH ratio to 1:1 (0.5 eq. of alcohol per Zn) decreased monomer conversion, highlighting the poor ability of the residual amido group on Zn to initiate the polymerization (entry 5).

At lower catalyst loading (0.2 mol % eq. of Zn), the bimetallic complex **5** lags behind the complex **4**, giving 86% conversion in 15 min, whereas the complex **4** has achieved full conversion in 5 min (Table 1, entries 6 and 7). At 0.1-mol % catalytic loading, the complex **4** has enabled complete monomer conversion in 5 min and 83% conversion in 3 min, ranking it as the most active monometallic Zn catalyst for LA ROP (TOF = 16,600 h^{-1}) (Table 1, entries 8 and 9). Here, narrowly dispersed PLA chains with the molar masses of 116,200 and 110,700 g·mol^{-1} have been obtained. Although high, these values are slightly lower than the theoretical ones, probably due to the presence of residual water in CH_2Cl_2 or lactide. A further comparison between **4** and **5** reveals that the mononuclear complex provides superior control of the PLA microstructure, particularly at lower catalyst loadings. To rationalize this outcome, we hypothesized that the initiation

https://doi.org/10.1021/acscatal.5c01335
ACS Catal. 2025, 15, 9117−9129

step for complex **5** does not proceed well at both metal centers simultaneously under increasingly dilute conditions and in the absence of a large excess of alcohol. The complexes **4** and **5** were subsequently tested under chain-transfer conditions, in the presence of 10 equivalents of alcohol and at the catalytic loading of 0.02 mol % (equivalents of Zn) (Table 1, entries 11−12). Under these conditions, the best performance was exhibited by the bimetallic complex **5**, yielding a narrow-disperse PLA with predictable M_n and 90% monomer conversion in 20 min (TOF = 13,500 h^{-1}), 10 min less than its monometallic counterpart. With the aim of obtaining more information on the ROP mechanism with the complexes **4** and **5**, PLA chain-end group analysis, alcoholysis experiments on the complexes, and kinetic studies were carried out. The MALDI-TOF MS spectrometric analysis of PLA samples produced either from **4** or **5** with ^{i}PrOH in a 1:1 ratio and 25 mol equivalents of LA (100% conversion, 1 min) showed in both cases isopropoxy-terminated chains with a peak spacing of 144 Da and some minor intercalated peaks due to trans-esterification reactions (see SI, Figures S47−S49). A kinetic study carried out with complexes **4** and **5** in CH_2Cl_2 at room temperature tends to confirm this hypothesis. The semi-logarithmic plot of *rac*-LA with time shows a linear relationship at different concentrations of complex **4**, indicating a first-order kinetic in monomer concentration (Figure 6a). The evolution of the M_n and $Đ$ values with conversion confirmed the well-controlled character of the polymerization. The slopes of the fitted lines of log k_{app} vs log[**4**] and k_{app} vs [**4**] indicate a first order in catalyst concentration and the rate constant k_p of 386 $M^{-1}.min^{-1}$, which is higher than those reported for the best monometallic Zn complexes described to date (Figure 6b and Figure S46a, S46c).[4] Polymerization with the bimetallic complex **5** proceeds with first-order dependence in monomer when using one equivalent of ^{i}PrOH (0.5 mol. eq. per Zn) and with second-order dependence in monomer when using one equivalent of co-initiator per Zn metal center (Figure 6c−d and Figure S46b). In the latter case, the dependence of ln k_{app} vs ln [**5**] was analyzed; it indicates a first order in the bimetallic complex **5**, giving a global kinetic law of the form: $-d[LA]/dt = k_p[\mathbf{5}]^1[LA]^2$. The first-order dependence on **5** and the second-order dependence on lactide strongly imply that the integrity of the bimetallic biguanide−Zn complex is preserved under catalytic conditions.[44]

We have attempted to prepare, isolate, and structurally characterize alkoxy-zinc biguanides, presumed to be the species responsible for the performance of the process. To generalize the results, the alcoholysis of all the complexes yields mixed oligomers of $\{[(Me_3Si)_2N]Zn\text{-}\mu^2\text{-}O^iPr\}_2$ or $[EtZn\text{-}\mu^3\text{-}O^iPr]_4$ along with **1** and **6** (the homoleptic zinc complex − for details, see SI, S32−S38). As homoleptic complex **6** is suspected to form under catalytic conditions, we performed the ROP of *rac*-LA in the presence of **6**. The results showed that it was active, but much less than **4** and **5**, producing PLA with only 10% conversion after 1 min at room temperature and with one molar % catalyst loading (Table S2, entry 16). It should be highlighted that the combination of $Zn[N(SiMe_3)_2]_2$ and alcohol has been previously described as an effective catalyst for the ROP of cyclic esters.[45] Therefore, we performed ROP tests using $Zn[N(SiMe_3)_2]_2$/^{i}PrOH (1:1), biguanide/^{i}PrOH (1:1) or a mixture of biguanide, $Zn[N(SiMe_3)_2]_2$ and ^{i}PrOH in a 1:1:1 ratio (Table S2, entries 17−19). All these combinations failed to match the performance of complexes **4** and **5**, in terms of both activity and polymerization control, indicating that the biguanide−Zn and Zn−biguanide−Zn entities are preserved under catalytic conditions and responsible for the catalytic activity.

In order to gain further insight into the mechanism of ROP with biguanide Zn complexes, we performed stochiometric reactions with complexes **2**, **4** and **5** with 2 or 5 equivalents of *L*-LA in CD_2Cl_2 and the subsequent addition of one equivalent of ^{i}PrOH (per metal). The NMR spectra of the complexes mixed with *L*-LA revealed negligible changes in chemical shifts of both components, indicating that interaction between the complexes and the monomer is weak. The NMR spectrum of mixture of complex **4** and *L*-LA, recorded 10 min after the addition of ^{i}PrOH, exhibited 90% conversion of *L*-LA to its oligomeric forms. The signals from the biguanide ligand get sharper than in **5** and free $HN(SiMe_3)_2$ was identified in solution (see SI, Figure S34). Similarly, **5** with 2 eq. of *L*-LA showed no interaction, and after the addition of ^{i}PrOH only signals attributed to opened oligomeric form of lactide and free amine were observed (see SI, Figure S35). The NMR spectrum of complex **2** mixed with *L*-LA and ^{i}PrOH also showed the complete alcoholysis of the complex but no conversion of LA (see SI, Figure S33). In light of these results and the blank ROP tests carried out with $Zn[N(SiMe_3)_2]_2$ and ^{i}PrOH, which show that the actual catalysts are not the oligomers of ′Zn, O^{i}Pr and $(Me_3Si)_2N$′ but rather biguanide-Zn species, it is suggested that the rate of decomposition of complexes **4** and **5** in the presence of ^{i}PrOH and a large excess of LA monomer is slow relative to the initiation of LA polymerization. PLA chains are terminated by an isopropoxyester end group, as determined by MALDI-TOF analysis. However, Zn−O^{i}Pr formation is not observed to occur immediately when one equivalent of ^{i}PrOH is added to complex **4** or **5**. This suggests that the initiation steps of the polymerization reaction should not occur via the alcoholysis of the bis(trimethylsilyamido) ligand and subsequent insertion of the lactide monomer into the Zn−O^{i}Pr bond. In the presence of complex **4** (or **5**), ^{i}PrOH, and LA, it is rather hypothesized that ^{i}PrOH would be activated by the N atom(s) of the bis(trimethylsilyamido) ligand(s), weakening the interaction between N and Zn and increasing the Lewis acidity of Zn. This would also activate LA by coordination toward the addition of ^{i}PrOH. After the initiation step, the bis(trimethylsilyl)amine would be released, and an ordinary coordination insertion mechanism could take place (see SI, Figure S36).

In order to get closer to industrial conditions, we preliminarily tested the thermal robustness of **5** in boiling toluene, in molten lactide at 130 °C as well as in the solid state at 160 °C, which showed significantly longer time of decomposition than that of polymerization. The polymerization of recrystallized technical grade *rac*-lactide was feasible with dodecanol as an initiator, exhibiting promising results, which will be the subject of our further studies.

The complexes **4** and **5** were also tested for the ROP of the more reluctant *rac*-*β*-butyrolactone (BL) monomer (see Table 2). Under optimized conditions, the complexes **4** and **5** exhibited moderate activity toward the ROP of BL, affording narrow-disperse PHB with 94% and 63% conversion, respectively, after 3 h at 45 °C in CH_2Cl_2 at 1 mol % catalyst loading.

Copolymers are considered appealing targets due to their potential to exhibit enhanced mechanical and/or thermal properties in comparison to the respective homopolymers.[10−28] To the best of our knowledge, di- or triblock

https://doi.org/10.1021/acscatal.5c01335
ACS Catal. 2025, 15, 9117−9129

Table 2. ROP of β-Butyrolactone and *co*ROP with Lactide Mediated by the Biguanide−Zn Complexes 4 and 5[a]

Entry	Cat.	$[M_1]_0:[M_2]_0:[M_3]_0:[cat]_0:[^iPrOH]$	M_1	M_2	M_3	T_1 [°C]	T_2 [°C]	T_3 [°C]	t_1 [min]	t_2	t_3 [min]	M_1 conv. [%][b]	M_2 conv. [%][b]	M_3 conv. [%][b]	$M_{n,theo}$ [c] [g mol^{-1}]	$M_{n,exp}$ [d] [g mol^{-1}]	$Đ$[d]
1	4	100:0:0:1:1	BL	-	-	45	-	-	180	-	-	94	-	-	8,800	6,200	1.04
2	5	100:0:0:0.5:1	BL	-	-	45	-	-	180	-	-	63	-	-	5,400	5,000	1.26
3	4	50:50:0:1:1	*L*-LA	BL	-	20	45	-	1	3 h	-	100	38	-	8,800	7,000	1.45
4	4	50:50:0:1:1	*L*-LA	BL	-	20	45	-	1	24 h	-	100	84	-	10,800	8,300	1.64
5	4	50:50:0:1:1	BL	*L*-LA	-	45	20	-	180	1 min	-	90	90	-	10,400	11,000	1.06
6	4	50:50:50:1:1	BL	*L*-LA	*D*-LA	45	20	20	210	15 min	25	93	99	91	17,700	14,000[e]	-
7	4	50:50:50:1:1	*rac*-LA	BL	*rac*-LA	20	45	20	2	5 h[f]	30	99	95	85	17,300	13,200	1.26
8	5	50:50:50:0.5:1	*rac*-LA	BL	*rac*-LA	20	45	20	2	40 h	360	99	93	95	18,000	16,000	1.29

[a]All reactions have been at least duplicated. Polymerization conditions: $[M]_0$ = 1.5 M, $[4]_0$ = 0.015 mM, CH_2Cl_2. [b]Monomer conversion. [c]Calculated using $M_{n,theo}$ = [*rac*-LA]$_0$/[^{i}PrOH]$_0$ × M_{LA} × Conv.$_{LA}$ + [*rac*-BL]$_0$/[^{i}PrOH]$_0$ × M_{BL} × Conv.$_{BL}$. [d]Measured by GPC on the crude reaction mixture without precipitation of the polymer in THF (45 °C) using PS standards and corrected by applying weighted correction factors (0.58 for PLA and 0.54 for PHB). [e]Determined by DOSY NMR. [f]Then left for 5 days.

copolymers from *L*-lactide, *D*-lactide and *rac*-lactide prepared by a sequential addition of monomers to the solution of primary polymer with homoleptic zinc complex bearing chelating amino-phenoxy ligand were reported only very recently.[19] Lactide copolymerization with β-butyrolactone feasible via an irreversible process driven sequentially by discrete combination of Zn and Y complexes was published by Robinson[9] during the completing of this work. Our successful result of β-butyrolactone and lactide polymerization led us to the idea to investigate one-pot synthesis of diblock copolymers (PHB-*b*-PLLA) with complex **4** by sequential addition of the two monomers. The addition of butyrolactone first, followed by *L*-lactide, proved to be more efficient than the reverse, leading to the diblock copolymer with BL and LA conversions of 90% after a sequence at 45 °C for 3 h for the ROP of BL and 1 min at 20 °C for LA. The GPC analysis of the copolymer chains thus formed showed a unimodal distribution, a narrow $Đ$ and the average molecular-weight number consistent with that calculated on the basis of the ratio of monomers and conversions (Figures S39−S45). DOSY (diffusion ordered spectroscopy) NMR analysis revealed a unique diffusion coefficient of 1.22 × 10^{-10} $m^2.s^{-1}$ ($CDCl_3$, 298 K), also consistent with the formation of copolymer chains rather than a mixture of homopolymers (Figure 7, Figures S38a−S38g in SI).

The average molecular weight, close to that found by GPC analysis, could be determined on the basis of DOSY calibration experiments ($M_{n,DOSY}$ = 10,300 g·mol^{-1}) (see SI, Table S4 and Figure S37). No trace resonances attributed to the PLA−PHB linking units were detected in ^{1}H NMR, that would attest the formation of only a diblock (PHB-*b*-PLA) without secondary transesterification reactions (Figure S32 in SI). The living nature of the polymerization was further confirmed by the addition of a third batch of 50 equivalents of *D*-LA, resulting in a PHB-*b*-PLLA-*b*-PDLA triblock *at*-sb-*st*-sb-*st* copolymer (Table 2, entry 6). The triblock copolymer was insoluble in THF, precluding GPC measurements in this solvent. Nevertheless, DOSY NMR analysis confirmed the formation of a unique triblock copolymer with a diffusion coefficient equal to 1.01 × 10^{-10} $m^2.s^{-1}$ ($CDCl_3$, 298 K) and the estimated M_n value of 14,000 g·mol^{-1} based on PLA-curve calibration (Figure 7 − lower panel). The ^{1}H NMR spectrum of the triblock copolymer shows a single quartet attributed to the methine (CH) signal of the two PLA stereoblocks, indicating that transesterification or *L*/*D* LA monomer scrambling events are minimal (Figure 8). In addition, we were able to prepare a triblock copolymer with PHB as the middle block. The incorporation of an atactic PLA chain instead of isotactic PLLA as the initial block did not impede the ROP of BL to the same extent as that observed in the synthesis of PLLA-*b*-PHB diblocks (Table 2, entries 7 and 4). GPC data show a unimodal profile with the M_n value being slightly lower than predicted and narrow dispersity ($Đ$ = 1.26). At last, the dinuclear complex **5** was also shown to be able to promote the formation of the PLA-*b*-PHB-*b*-PLA triblock, although longer reaction times were required to build the last two PHB and PLA blocks. All of these results showed the ability of both complexes **4** and **5** to promote the synthesis of diblock and/or triblock copolymers in a controlled and living manner.

CONCLUSIONS

Mono- and dizinc complexes with the cheap, easily accessible, and structurally versatile ditopic biguanide proligand **1** were

https://doi.org/10.1021/acscatal.5c01335
ACS Catal. 2025, 15, 9117−9129

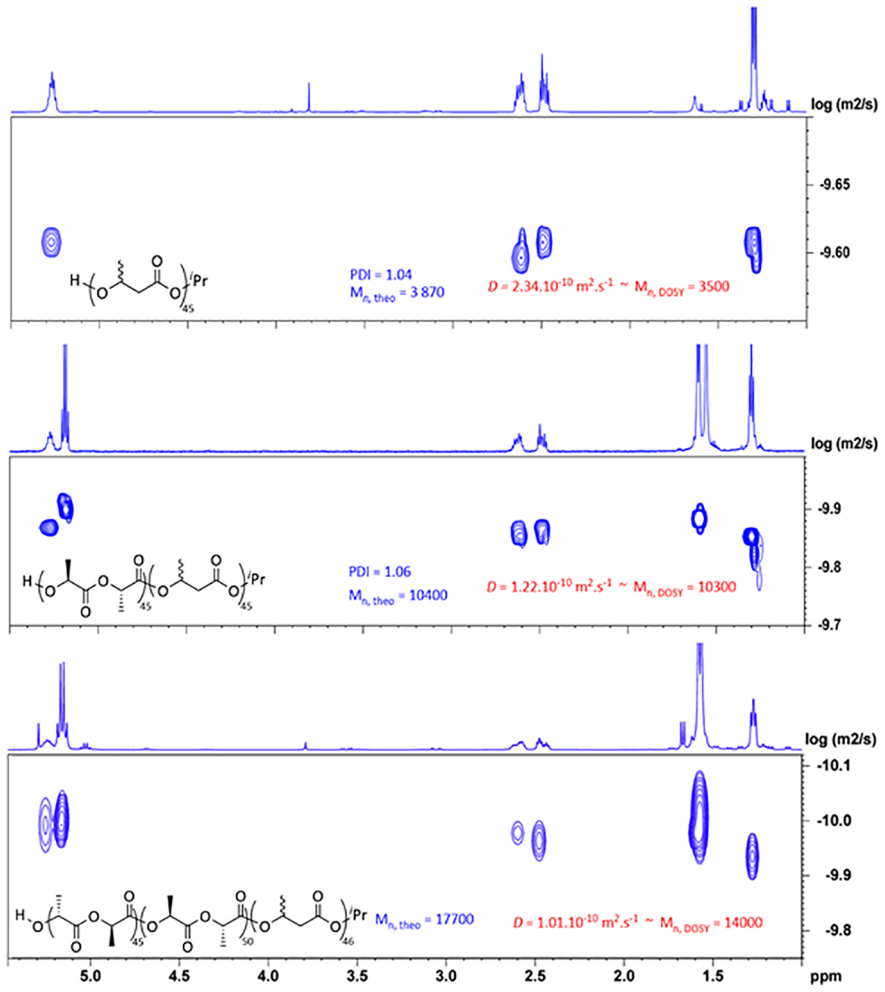

Figure 7. DOSY NMR spectra of PHB (upper panel), PLLA-*b*-PHB (middle panel, Table 2, entry 5) and PDLA-*b*-PLLA-*b*-PHB (lower panel – Table 2, entry 6) in $CDCl_3$.

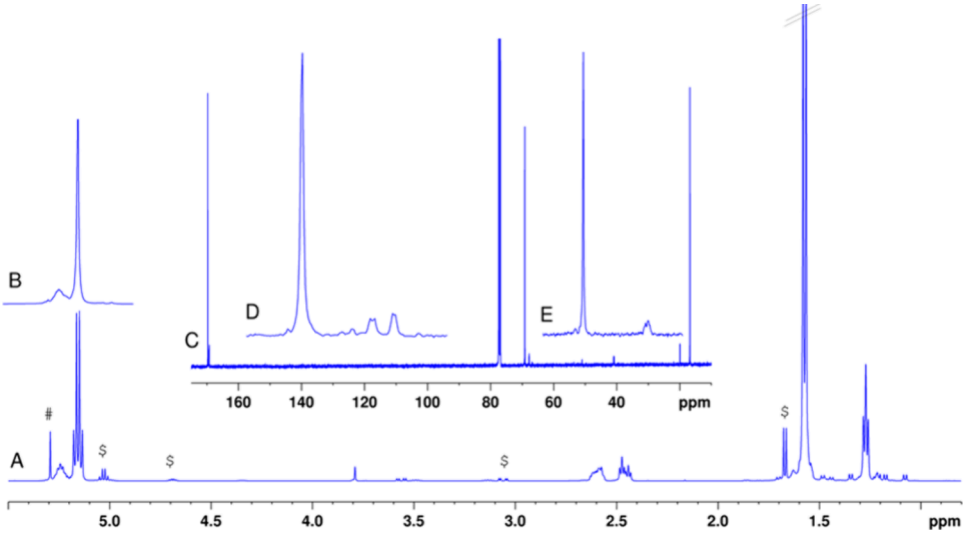

Figure 8. ^{1}H (A), 1D-^{1}H selective decoupled (B) and ^{13}C NMR spectra (C) with details of the carbonyl (D) and methine regions (E) of a crude mixture of PHB-*b*-PLLA-*b*-PDLA (Table 2, entry 6) in $CDCl_3$. Unreacted monomers ($) and CH_2Cl_2 (#) are marked.

synthesized by a one-step protocol. While the ethylzinc complexes **2** and **3** are inactive in the ROP of *rac*-lactide, the performance of the zinc amides **4** and **5** is striking after their activation by ^{i}PrOH: *i)* the highest TOF number 16,600 h^{-1} for **4** and 13,500 h^{-1} for **5**; *ii)* very high M_n under mild polymerization conditions (the highest value of 116,200 g·mol^{-1} for **4** and 67,100 g·mol^{-1} for **5**; *iii)* narrow polydispersity values. Based on the most independent, comparable and

https://doi.org/10.1021/acscatal.5c01335
ACS Catal. 2025, 15, 9117−9129

valuable criterion, the rate constant k_p, their catalytic performance, (k_p(25 °C) of 386 $M^{-1}.min^{-1}$ for **4** and 237 $M^{-2}.min^{-1}$ for **5**), exceeds the highest value reported by Robinson[4] (~300 $M^{-1}.min^{-1}$, Figure S46c, SI). These observations assign **4** and **5** the role of some of the most efficient catalysts when the lactide ROP is activated by ^{i}PrOH. Because of the structurally versatile behavior of the biguanide ligand, complex **5** undergoes a possible mutual interchange of the positions of zinc atoms, which is in contrast to monometallic **4** or bimetallic **3** with the Zn atom position locked to the "BDI" side. This could explain the ability of this "nonsymmetrical" bimetallic complex to promote the ROP of LA at both Zn sites, either at the same time or consecutively, to form PLA chains with a unimodal molecular-weight distribution. Complex **5** seems also suitable for industrial conditions as evidenced by preliminary tests in boiling toluene and molten *rac*-lactide.

Successful consecutive living copolymerization of *β*-butyrolactone with either *L*-, *D*- or *rac*-lactide giving di- and triblock copolymers with narrow dispersity opens the door to the preparation of various di- or oligoblock heterocopolymers. Most surprisingly, these processes are performed with only one portion of the zinc complex and alcohol; after the completion of each step, it is only necessary to change the monomers and eventually the temperature. In comparison with the recent literature,[9] in order to achieve a similar copolymer (but only diblock), it was necessary to add two different catalysts with different metals and ligands plus monomers in a batch process at elevated temperature.

MATERIALS AND METHODS

All solvents and chemical reagents were purchased from commercial sources and used without further purification. Some synthetic procedures were performed using the standard Schlenk techniques under an inert argon atmosphere (99.999%) (inert gas was passed through the oxygen/moisture trap Supelco before entering the vacuum/inert line), and solvents were dried with the help of solvent purification system PureSolv MD 7 supplied by Innovative Technology, Inc., degassed, and then stored under argon atmosphere over a potassium or sodium mirror, if needed. Synthetic protocols and characterization of **1**−**6** are given in detail in SI file p. S51 − S56. Single crystals suitable for X-ray analyses were obtained from the corresponding saturated solutions of products in organic solvent(s) cooled to 7 or −30 °C or by slow evaporation at room temperature. Deuterated solvents for NMR spectroscopy were distilled, degassed, and stored over a K or Na mirror under an argon atmosphere. Elemental analyses (C, H, and N) were performed on an automatic microanalyzer Flash 2000 Organic elemental analyzer. Mass spectra of PLA samples were acquired on a time-of-flight mass spectrometer (MALDI-ToF-Microflex LRF, Bruker Daltonics). An external quadratic multipoint calibration was carried out before each measurement using polyethylene glycol (PEG) mixed in THF with dithranol (DIT). Analysis was performed with DIT as the matrix (10 mg/mL) and sodium trifluoroacetate (10 mg/mL) as an additive. The polymer (10 mg/mL), the matrix, and the additive were mixed in a volumetric ratio of 1/1/0.5 in THF. All the analyses were performed in positive reflectron mode.

NMR Spectroscopy. NMR spectra were recorded from solutions of appropriate compounds in deuterated solvent(s) on a Bruker Avance 500 spectrometer (equipped with a Z-gradient 5 mm Prodigy cryoprobe) at frequencies for ^{1}H (500.13 MHz) or ^{13}C{^{1}H} (125.76 MHz) or a Bruker UltraShield 400 spectrometer at frequencies for ^{1}H (400.13 MHz), ^{13}C{^{1}H} (100.62 MHz) at 295 K or in some cases at various temperatures. Low-temperature NMR experiments of Zn complex **5** were performed on a Bruker Avance II spectrometer with a triple resonance broad-band probe (5 mm TBO BB-1*H*/19F/D Z-GRD) operating at 499.9 MHz for ^{1}H and 125.7 MHz for ^{13}C. Solutions were obtained by dissolving approximately 40 mg of each compound in approximately 0.6 mL of deuterated solvents. Values of ^{1}H chemical shifts were referenced to residual signals of benzene ($\delta(^{1}H)$ = 7.16), tetrahydrofuran ($\delta(^{1}H)$ = 1.73) or toluene ($\delta(^{1}H)$ = 2.09). Values of ^{13}C chemical shifts were calibrated to signals of benzene ($\delta(^{13}C)$ = 128.4), tetrahydrofuran ($\delta(^{13}C)$ = 67.6), or toluene ($\delta(^{13}C)$ = 20.4). All ^{13}C NMR spectra were measured using a standard proton-decoupled experiment, and CH/CH_3 vs C_q/CH_2 were sometimes differentiated with the APT method's help.[46] NMR signal assignment was supported by ^{1}H, ^{1}H−COSY, ^{1}H, ^{1}H-NOESY, ^{1}H, ^{13}C-HSQC or ^{1}H, ^{13}C-HMBC 2D spectra. The DOSY spectra were recorded on a Bruker Avance III HD 600 spectrometer equipped with an ATMA BBOF 5 mm Cryoprobe with a *z*-axis gradient coil operating at 600.13 MHz (^{1}H). The maximum gradient strength was 65.8 G/cm. The DOSY spectra were acquired in 5 mm NMR tubes, and all the experiments were performed at 25 °C and without sample spinning to avoid convection. All DOSY experiments were performed using standard Bruker pulse sequence - *dstebpgp3s* - a double stimulated echo sequence with bipolar gradient pulses and three spoil gradients with convection compensation. The diffusion time was 0.1 s (D). The duration of the magnetic field pulse gradients was adjusted for each polymer in a range of 500−2000 ms (d/2). The delay for gradient recovery was 0.2 ms, and the eddy current delay 5 ms. For each DOSY-NMR experiment, a series of 16 spectra on 32 K data points were collected. The pulse gradients were incremented from 2% to 98% of the maximum gradient strength in a linear ramp with a total experiment time of 23 min. The temperature was set and controlled at 295 K with an air flow of 400 L/h in order to avoid any temperature fluctuations due to sample heating during the magnetic field pulse gradients. After Fourier transformation and baseline correction, the diffusion dimension was processed with Topspin 3.6.1 software and Dynamic Center 2.4.4. Stokes−Einstein equation: $D = b'M^{-\nu}$ (b', ν = constant) is used to determined molecular molar mass of polymers via the diffusion coefficient.[47]

Crystallography. The X-ray data for colorless crystals of all complexes were obtained at 150 K using Oxford Cryostream low-temperature device with a Bruker D8-Venture diffractometer equipped with Mo (Mo/K_α radiation; λ = 0.71073 Å) microfocus X-ray (IμS) source, Photon CMOS detector, and Oxford Cryosystems cooling device was used for data collection. Obtained data were treated by XT-version 2014/5 and SHELXL-2017/1 software implemented in APEX3 v2016.9−0 (Bruker AXS) system.[48] $R_{int} = \Sigma|F_0^2 - F_{o,mean}^2|/\Sigma F_0^2$, $S = [\Sigma(w(F_0^2 - F_c^2)^2)/(N_{diffrs} - N_{params})]^{1/2}$ for all data, $R(F) = \Sigma||F_0| - |F_c||/\Sigma|F_0|$for observed data, $wR(F^2) = [\Sigma(w(F_0^2 - F_c^2)^2)/(\Sigma w(F_0^2)^2)]^{1/2}$ for all data. Crystallographic data for all structural analysis have been deposited with the Cambridge Crystallographic Data Centre, CCDC nos. 2120578, 2377227−2377231. Copies of this information may be obtained free of charge from The Director, CCDC, 12 Union Road, Cambridge CB2 1EY, UK (fax: + 44−1223−

https://doi.org/10.1021/acscatal.5c01335
ACS Catal. 2025, 15, 9117−9129

336033; e-mail: deposit@ccdc.cam.ac.uk or www: http://www.ccdc.cam.ac.uk). The frames for all complexes were integrated with the Bruker SAINT software package using a narrow-frame algorithm. Data were corrected for absorption effects using the multiscan method (SADABS). The structures were solved and refined by using the Bruker SHELXTL Software Package.

Hydrogen atoms were mostly localized on a difference Fourier map; however, to ensure uniformity of treatment of crystal, most of the hydrogen atoms were recalculated into idealized positions (riding model) and assigned temperature factors $H_{iso}(H)$ = 1.2 Ueq (pivot atom) or of $1.5U_{eq}$ (methyl). H atoms in methyl, methylene, methine moieties and C−H in aromatic rings were placed with C−H distances of 0.96, 0.97, 0.98 and 0.93Å. Hydrogen atoms in NH groups were added freely according to the maxima on the difference Fourier map. In **6**, four disordered *n*-hexane molecules were masked by the SQUEEZE[49] program.

DFT Calculations. All the calculations were performed with the Gaussian 16 program.[50] The geometries of all compounds and their selected isomers as well as by products and starting materials were fully optimized at B3LYP/6−311+G(d,p), level of theory[51,52] without any structure simplifications. The structures of complexes obtained by X-ray diffraction were mostly used as the input structures. The conductor-like polarizable continuum model (CPCM)[53] was employed for the solvation effects (THF, benzene). The empirical dispersion correction D3 was applied for all structures.[54] All of the structures are minima on the potential energy surface, as confirmed by the frequency calculations at the same level of theory and transition states by only one imaginary frequency. The topological analysis of the theoretical function $\rho(r)$ was performed using the AIMAll program package.[55] Within the framework of Atoms in Molecules theory, the atomic charges in all compounds together with bond, ring and cluster critical points were calculated, the interaction energies within the critical points were calculated according to Espinosa's equation.[56] The total enthalpies and Gibbs free energies were calculated at T = 298.15 K. The NMR parameters were calculated by GIAO method.[57] Appropriate Cartesian coordinates for all computed structures are given in separate files. The visualization of the transition state in a "pendulum"-like equilibrium is attached as gif file.

Typical PLA Synthesis Procedure in Solution. Under argon atmosphere, to a solution of *rac*-lactide (288.3 mg; 100 eq.; 2.00 mmol) in the chosen solvent (1.3 mL; $[LA]_0$ = 1.50 M), 1 eq. of catalyst and 1 eq. of co-initiator ^{i}PrOH (1.53 μL; 0.02 mmol) were added. The vial was crimped and allowed to stir at the desired temperature. The reaction vial was opened to the air in order to quench the reaction. The conversion was determined by ^{1}H NMR spectroscopy and the molar mass and dispersity by Gel Permeation Chromatography (GPC). The provided PLA was washed with methanol in order to remove the residual monomer and catalyst.

Typical PHB Synthesis Procedure in Solution. Under argon atmosphere, to a solution of *rac*-β-butyrolactone (0.1 mL; 100 eq.; 1.23 mmol) in the chosen solvent (0.8 mL; $[BL]_0$ = 1.50 M), 1 eq. of catalyst and 1 eq. of co-initiator - ^{i}PrOH (0.94 μL; 0.01 mmol) were added. The vial was crimped and allowed to remain under stirring at the desired temperature. The reaction vial was opened to air in order to quench the reaction. The conversion was determined by ^{1}H NMR spectroscopy, and the molar mass and dispersity were determined by GPC.

Typical PHB-*b*-PLLA Synthesis Procedure in Solution. Under argon atmosphere, to a solution of *rac*-β-butyrolactone (0.1 mL; 50 eq.; 1.23 mmol) in DCM (0.8 mL; $[BL]_0$ = 1.50 M), 1 eq. of catalyst and 1 eq. of co-initiator ^{i}PrOH (1.88 μL; 0.02 mmol) were added. The vial was crimped and allowed under stirring at 45 °C for 3 h. After, a solution of *L*-lactide (177.3 mg; 50 eq.; 1.23 mmol) in DCM (0.8 mL; $[LA]_0$ = 0.75 M) was added to the reaction. The vial was closed and left under stirring at 25 °C for 1 min. The reaction vial was opened to air in order to quench the reaction. The conversion was determined by ^{1}H NMR spectroscopy and the molar mass and dispersity by GPC and DOSY NMR analysis.

Typical PLLA-*b*-PHB Synthesis Procedure in Solution. Under argon atmosphere, to a solution of *L*-lactide (177.3 mg; 50 eq.; 1.23 mmol) in DCM (0.8 mL; $[LA]_0$ = 1.50 M), 1 eq. of catalyst and 1 eq. of co-initiator ^{i}PrOH (1.88 μL; 0.02 mmol) were added. The vial was closed and left under stirring at 25 °C for 1 min. After, a solution of *rac*-β-butyrolactone (0.1 mL; 50 eq.; 1.23 mmol) in DCM (0.8 mL; $[BL]_0$ = 0.75 M) was added to the reaction. The vial was crimped and allowed to stir at 45 °C for the desired time. The reaction vial was opened to air in order to quench the reaction. The conversion was determined by ^{1}H NMR spectroscopy and the molar mass and dispersity by GPC and DOSY NMR analysis.

Typical PHB-*b*-PLLA-*b*-PDLA Synthesis Procedure in Solution. Under argon atmosphere, to a solution of *rac*-β-butyrolactone (81.5 μL; 50 eq.; 1.00 mmol) in DCM (1.0 mL; $[BL]_0$ = 1.00 M), 1 eq. of catalyst and 1 eq. of co-initiator ^{i}PrOH (0.76 μL; 0.01 mmol) were added. The vial was crimped and allowed to stir under stirring at 45 °C for 3.5 h. After, a solution of *L*-lactide (144.1 mg; 50 eq.; 1.00 mmol) in DCM (1.0 mL; $[LA]_0$ = 0.50 M) was added to the reaction. The vial was closed and left under stirring at 25 °C for 15 min. Afterward, a solution of *D*-lactide (144.1 mg; 50 eq.; 1.00 mmol) in DCM (1.0 mL; $[LA]_0$ = 0.33 M) was added to the reaction. The vial was closed and left under stirring at 25 °C for 25 min. The reaction vial was opened to air in order to quench the reaction. The conversion was determined by ^{1}H NMR spectroscopy and the molar mass by DOSY NMR analysis.

Typical PLA-*b*-PHB-*b*-PLA Synthesis Procedure in Solution. Under argon atmosphere, to a solution of *rac*-lactide (144.1 mg; 50 eq.; 1.00 mmol) in DCM (1.0 mL; $[LA]_0$ = 1.00 M), 1 or 0.5 eq. of catalyst and 1 eq. of co-initiator ^{i}PrOH (0.76 μL; 0.01 mmol) were added. The vial was crimped and allowed to stir at 25 °C for 2 min. After, a solution of rac-β-butyrolactone (81.5 μL; 50 eq.; 1.00 mmol) in DCM (1.0 mL; $[BL]_0$ = 0.50 M) was added to the reaction. The vial was crimped and let under stirring at 45 °C for the desired time. After, a solution of *rac*-lactide (144.1 mg; 50 eq.; 1.00 mmol) in DCM (1.0 mL; $[LA]_0$ = 0.33 M) was added to the reaction. The vial was closed and allowed to stir at 25 °C for the desired time. The reaction vial was opened to air in order to quench the reaction. The conversion was determined by ^{1}H NMR spectroscopy and the molar mass and dispersity by GPC and DOSY NMR analysis.

■ ASSOCIATED CONTENT

Supporting Information

The Supporting Information is available free of charge at https://pubs.acs.org/doi/10.1021/acscatal.5c01335.

https://doi.org/10.1021/acscatal.5c01335
ACS Catal. 2025, 15, 9117−9129

mol files (ZIP)
X-ray data (CIF)
Synthetic procedures and structural issues of ligand and complexes, reactivity studies, polymerization results, NMR spectra, crystallographic parameters, computational methods (PDF)

AUTHOR INFORMATION

Corresponding Authors

Tomáš Chlupatý − *Department of General and Inorganic Chemistry, Faculty of Chemical Technology, University of Pardubice, Pardubice 532 10, Czech Republic;* orcid.org/0000-0002-0883-5593; Email: tomas.chlupaty@upce.cz

Pierre Le Gendre − *Univ. Bourgogne Europe, Institut de Chimie Moléculaire de l'Université de Bourgogne (ICMUB), 21078 Dijon, France;* orcid.org/0000-0003-2635-5216; Email: pierre.le-gendre@u-bourgogne.fr

Aleš Růžička − *Department of General and Inorganic Chemistry, Faculty of Chemical Technology, University of Pardubice, Pardubice 532 10, Czech Republic;* orcid.org/0000-0001-8191-0273; Email: ales.ruzicka@upce.cz

Authors

Benjamin Théron − *Univ. Bourgogne Europe, Institut de Chimie Moléculaire de l'Université de Bourgogne (ICMUB), 21078 Dijon, France*

Lukáš Vlk − *Department of General and Inorganic Chemistry, Faculty of Chemical Technology, University of Pardubice, Pardubice 532 10, Czech Republic*

Marie-José Penouilh − *Univ. Bourgogne Europe, Institut de Chimie Moléculaire de l'Université de Bourgogne (ICMUB), 21078 Dijon, France*

Eliška Procházková − *Institute of Organic Chemistry and Biochemistry, Czech Academy of Sciences, Prague 160 00, Czech Republic;* orcid.org/0000-0002-4768-3422

Raluca Malacea-Kabbara − *Univ. Bourgogne Europe, Institut de Chimie Moléculaire de l'Université de Bourgogne (ICMUB), 21078 Dijon, France*

Complete contact information is available at: https://pubs.acs.org/10.1021/acscatal.5c01335

Author Contributions

[§]B.T. and L.V. contributed equally. B.T.: investigation, ROP catalysis; L.V.: investigation, synthesis, ROP catalysis, writing; T.C.: investigation, synthesis, catalysis, NMR spectroscopy, writing; E.P.: VT NMR, writing; M.-J.P.: DOSY NMR; R.M.-K.: conceptualization, supervision, writing; P.L.G.: conceptualization, supervision, writing; A.R.: conceptualization, supervision, X-ray diffraction analysis, calculations, writing. The manuscript was written through contributions of all authors. All authors have given approval to the final version of the manuscript.

Notes

The authors declare no competing financial interest.

ACKNOWLEDGMENTS

This work was supported by the Czech Science Foundation grant no. 21-02964S. Research infrastructure project CZ.02.01.01/00/23_021/0008593 (Innovative materials suitable for high added value applications (INMA)) and a bilateral Czech-French project PHC BARRANDE 2024 50539QG are acknowledged.

REFERENCES

(1) Haider, T. P.; Völker, C.; Kramm, J.; Landfester, K.; Wurm, F. R. Plastics of the Future? The Impact of Biodegradable Polymers on the Environment and on Society. *Angew. Chem., Int. Ed.* **2019**, *58*, 50−62.

(2) Ramezani Dana, H.; Ebrahimi, F. Synthesis, properties, and applications of polylactic acid-based polymers. *Polym. Eng. Sci.* **2023**, *63*, 22−43.

(3) Cheng, M.; Attygalle, A. B.; Lobkovsky, E. B.; Coates, G. W. Single-Site Catalysts for Ring-Opening Polymerization: Synthesis of Heterotactic Poly(lactic acid) from *rac*-Lactide. *J. Am. Chem. Soc.* **1999**, *121*, 11583−11584.

(4) Chellali, J. E.; Alverson, A. K.; Robinson, J. R. Zinc Aryl/Alkyl *β*-diketiminates: Balancing Accessibility and Stability for High-Activity Ring-Opening Polymerization of *rac*-Lactide. *ACS Catal.* **2022**, *12*, 5585−5594.

(5) Thevenon, A.; Romain, C.; Bennington, M. S.; White, A. J. P.; Davidson, H. J.; Brooker, S.; Williams, C. K. Dizinc Lactide Polymerization Catalysts: Hyperactivity by Control of Ligand Conformation and Metallic Cooperativity. *Angew. Chem.* **2016**, *55*, 8680−8685.

(6) Coles, M. P.; Hitchcock, P. B. Zinc Guanidinate Complexes and Their Application in Ring-Opening Polymerisation Catalysis. *Eur. J. Inorg. Chem.* **2004**, *2004*, 2662−2672.

(7) D'Auria, I.; Ferrara, V.; Tedesco, C.; Kretschmer, W.; Kempe, R.; Pellecchia, C. Guanidinate Zn(II) Complexes as Efficient Catalysts for Lactide Homo- and Copolymerization under Industrially Relevant Conditions. *ACS Appl. Polym. Mater.* **2021**, *3*, 4035−4043.

(8) Suo, H.; Liu, S.; Liu, J.; Zhang, Z.; Qu, R.; Gu, Y.; Qin, Y. Novel epoxide-promoted polymerization of lactides mediated by a zinc guanidine complex: a potential strategy for the tin-free PLA industry. *Polym. Chem.* **2023**, *14*, 4652−4658.

(9) Chellali, J. E.; Woodside, A. J.; Yu, Z.; Neogi, S.; Külaots, I.; Guduru, P. R.; Robinson, J. R. Access to Stereoblock Polyesters *via* Irreversible Chain-Transfer Ring-Opening Polymerization (ICT-ROP). *J. Am. Chem. Soc.* **2024**, *146*, 11562−11569.

(10) Diaz, C.; Mehrkhodavandi, P. Strategies for the synthesis of block copolymers with biodegradable polyester segments. *Polym. Chem.* **2021**, *12*, 783−806.

(11) Aluthge, D. C.; Xu, C.; Othman, N.; Noroozi, N.; Hatzikiriakos, S. G.; Mehrkhodavandi, P. PLA-PHB-PLA Triblock Copolymers: Synthesis by Sequential Addition and Investigation of Mechanical and Rheological Properties. *Macromolecules* **2013**, *46*, 3965−3974.

(12) Xu, C.; Yu, I.; Mehrkhodavandi, P. Highly controlled immortal polymerization of *β*-butyrolactone by a dinuclear indium catalyst. *Chem. Commun.* **2012**, *48*, 6806−6808.

(13) Yu, I.; Ebrahimi, T.; Hatzikiriakos, S. G.; Mehrkhodavandi, P. Star-shaped PHB-PLA block copolymers: immortal polymerization with dinuclear indium catalysts. *Dalton Trans.* **2015**, *44*, 14248−14254.

(14) Ebrahimi, T.; Aluthge, D. C.; Patrick, B. O.; Hatzikiriakos, S. G.; Mehrkhodavandi, P. Air- and Moisture-Stable Indium Salan Catalysts for Living Multiblock PLA Formation in Air. *ACS Catal.* **2017**, *7*, 6413−6418.

(15) Rosen, T.; Goldberg, I.; Navarra, W.; Venditto, V.; Kol, M. Divergent [{ONNN}Mg-Cl] complexes in highly active and living lactide polymerization. *Chem. Sci.* **2017**, *8*, 5476−5481.

(16) Rosen, T.; Goldberg, I.; Venditto, V.; Kol, M. Tailor-Made Stereoblock Copolymers of Poly(lactic acid) by a Truly Living Polymerization Catalyst. *J. Am. Chem. Soc.* **2016**, *138*, 12041−12044.

(17) Sanchez, L. A. H.; Woroch, C. P.; Dumas, D. M.; Waymouth, R. M.; Kanan, M. W. Toughening Poly(lactic acid) without Compromise - Statistical Copolymerization with a Bioderived Bicyclic Lactone. *J. Am. Chem. Soc.* **2025**, *147*, 5212−5219.

(18) D'Auria, I.; D'Alterio, M. C.; Tedesco, C.; Pellecchia, C. Tailor-made block copolymers of L-, D- and rac-lactides and *ε*-caprolactone via one-pot sequential ring opening polymerization by pyridylamidozinc(II) catalysts. *RSC Adv.* **2019**, *9*, 32771−32779.

(19) Pongpanit, T.; Saeteaw, T.; Chumsaeng, P.; Chasing, P.; Phomphrai, K. Highly Active Homoleptic Zinc and Magnesium

Complexes Supported by Constrained Reduced Schiff Base Ligands for the Ring-Opening Polymerization of Lactide. *Inorg. Chem.* **2021**, *60*, 17114−17122.
(20) Chisholm, M. H.; Gallucci, J. C.; Phomphrai, K. Comparative Study of the Coordination Chemistry and Lactide Polymerization of Alkoxide and Amide Complexes of Zinc and Magnesium with a β-Diiminato Ligand Bearing Ether Substituents. *Inorg. Chem.* **2005**, *44*, 8004−8010.
(21) Kernbichl, S.; Reiter, M.; Mock, J.; Rieger, B. Terpolymerization of β-Butyrolactone, Epoxides, and CO_2: Chemoselective CO_2-Switch and Its Impact on Kinetics and Material Properties. *Macromolecules* **2019**, *52*, 8476−8483.
(22) Fagerland, J.; Finne-Wistrand, A.; Pappalardo, D. Modulating the thermal properties of poly(hydroxybutyrate) by the copolymerization of *rac*-β-butyrolactone with lactide. *New J. Chem.* **2016**, *40*, 7671−7679.
(23) García-Valle, F. M.; Tabernero, V.; Cuenca, T.; Mosquera, M. E. G.; Cano, J.; Milione, S. Biodegradable PHB from *rac*-β-Butyrolactone: Highly Controlled ROP Mediated by a Pentacoordinated Aluminum Complex. *Organometallics* **2018**, *37*, 837−840.
(24) García-Valle, F. M.; Cuenca, T.; Mosquera, M. E. G.; Milione, S.; Cano, J. Ring-Opening Polymerization (ROP) of cyclic esters by a versatile aluminum Diphenoxyimine Complex: From polylactide to random copolymers. *Eur. Polym. J.* **2020**, *125*, 109527−109535.
(25) Zheng, X.-X.; Wang, Z.-X. Synthesis of aluminum complexes supported by 2-(1,10-phenanthrolin-2-yl)phenolate ligands and their catalysis in the ring-opening polymerization of cyclic esters. *RSC Adv.* **2017**, *7*, 27177−27188.
(26) Platel, R. H.; Hurst, A. R. Precise Microstructure Control in Poly(hydroxybutyrate-*co*-lactic Acid) Copolymers Prepared by an Yttrium Amine Bis(phenolate) Complex. *Macromolecules* **2020**, *53*, 10773−10784.
(27) Jeffery, B. J.; Whitelaw, E. L.; Garcia-Vivo, D.; Stewart, J. A.; Mahon, M. F.; Davidson, M. G.; Jones, M. D. Group 4 initiators for the stereoselective ROP of *rac*-β-butyrolactone and its copolymerization with *rac*-lactide. *Chem. Commun.* **2011**, *47*, 12328−12330.
(28) Whitehorne, T. J. J.; Schaper, F. Lactide, β-butyrolactone, δ-valerolactone, and ε-caprolactone polymerization with copper diketiminate complexes. *Can. J. Chem.* **2014**, *92*, 206−214.
(29) Chlupatý, T.; Nevoralová, J.; Růžičková, Z.; Růžička, A. Lithium and Dilithium Guanidinates, a Starter Kit for Metal Complexes Containing Various Mono- and Dianionic Ligands. *Inorg. Chem.* **2020**, *59*, 10854−10865.
(30) Bailey, C. J. Metformin: historical overview. *Diabetologia.* **2017**, *60*, 1566−1576.
(31) Viollet, B.; Guigas, B.; Garcia, N. S.; Leclerc, J.; Foretz, M.; Andreelli, F. Cellular and molecular mechanisms of metformin: an overview. *Clin. Sci.* **2012**, *122*, 253−270.
(32) Foretz, M.; Guigas, B.; Bertrand, L.; Pollak, M.; Viollet, B. Metformin: From Mechanisms of Action to Therapies. *Cell Metab.* **2014**, *20*, 953−966.
(33) Kathuria, D.; Raul, A. D.; Wanjari, P.; Bharatam, P. V. Biguanides: Species with versatile therapeutic applications. *Eur. J. Med. Chem.* **2021**, *219*, 113378−113416.
(34) Peddarao, T.; Sarkar, N.; Nembenna, S. Mono- and Bimetallic Aluminum Alkyl, Alkoxide, Halide and Hydride Complexes of a Bulky Conjugated Bis-Guanidinate(CBG) Ligand and Aluminum Alkyls as Precatalysts for Carbonyl Hydroboration. *Inorg. Chem.* **2020**, *59*, 4693−4702.
(35) Sahoo, R. K.; Sarkar, N.; Nembenna, S. Zinc Hydride Catalyzed Chemoselective Hydroboration of Isocyanates: Amide Bond Formation and C = O Bond Cleavage. *Angew. Chem., Int. Ed.* **2021**, *60*, 11991−12000.
(36) Peddarao, T.; Baishya, A.; Sarkar, N.; Acharya, R.; Nembenna, S. Conjugated Bis-Guanidines (CBGs) as β-Diketimine Analogues: Synthesis, Characterization of CBGs/Their Lithium Salts and CBG Li Catalyzed Addition of B-H and TMSCN to Carbonyls. *Eur. J. Inorg. Chem.* **2021**, *2021*, 2034−2046.
(37) Sahoo, R. K.; Mahato, M.; Jana, A.; Nembenna, S. Zinc Hydride Catalyzed Hydrofuntionalization of Ketones. *J. Org. Chem.* **2020**, *85*, 11200−11210.
(38) Glöckler, E.; Ghosh, S.; Schulz, S. β-Diketiminate and β-Ketoiminate Metal Catalysts for Ring-Opening Polymerization of Cyclic Esters. *Polym. Rev.* **2023**, *63*, 478−514.
(39) Webster, R. L. β-Diketiminate complexes of the first row transition metals: applications in catalysis. *Dalton Trans.* **2017**, *46*, 4483−4498.
(40) Sarish, S. P.; Nembenna, S.; Nagendran, S.; Roesky, H. W. Chemistry of Soluble β-Diketiminatoalkaline-Earth Metal Complexes with M-X Bonds (M = Mg, Ca, Sr; X = OH, Halides, H). *Acc. Chem. Res.* **2011**, *44*, 157−170.
(41) Bourget-Merle, L.; Lappert, M. F.; Severn, J. R. The Chemistry of β-Diketiminatometal Complexes. *Chem. Rev.* **2002**, *102*, 3031−3066.
(42) Thakur, M. S.; Singh, N.; Sharma, A.; Rana, R.; Abdul Syukor, A.R.; Naushad, M.; Kumar, S.; Kumar, M.; Singh, L. Metal coordinated macrocyclic complexes in different chemical transformations. *Coord. Chem. Rev.* **2022**, *471*, 214739.
(43) Tian, D.; Xie, Q.; Yan, L.; Tong, H.; Zhou, M. Zinc and aluminum complexes derived from 2,4-*N*, *N*′-disubstituted 1,3,5-triazapentadienyl ligands: Synthesis, characterization and catalysis of the ring-opening polymerization of *rac*-lactide. *Inorg. Chem. Commun.* **2015**, *58*, 35−38.
(44) Wu, J.-C.; Huang, B.-H.; Hsueh, M.-L.; Lai, S.-L.; Lin, C.-C. Ring-opening polymerization of lactide initiated by magnesium and zinc alkoxides. *Polymer* **2005**, *46*, 9784−9792.
(45) Yuan, Y.; Jing, X.; Xiao, H.; Chen, X.; Huang, Y. Zinc-based catalyst for the ring-opening polymerization of cyclic esters. *J. Appl. Polym. Sci.* **2011**, *121*, 2378−2385.
(46) Patt, S.; Shoolery, J. N. Attached proton test for carbon-13 NMR. *J. Magn. Reson.* **1982**, *46*, 535−539.
(47) Voorter, P.; McKay, A.; Dai, J.; Paravagna, O.; Cameron, N. R.; Junkers, T. Solvent-Independent Molecular Weight Determination of Polymers Based on a Truly Universal Calibration. *Angew. Chem., Int. Ed.* **2022**, *61*, No. e202114536.
(48) Sheldrick, G. M. SHELXT - Integrated space-group and crystal-structure determination. *Acta Crystallogr.* **2015**, *A71*, 3−8.
(49) Spek, A. L. PLATON SQUEEZE: a tool for the calculation of the disordered solvent contribution to the calculated structure factors. *Acta Crystallogr.* **2015**, *C71*, 9−18.
(50) Frisch, M. J.; Trucks, G. W.; Schlegel, H. B.; Scuseria, G. E.; Robb, M. A.; Cheeseman, J. R.; Scalmani, G.; Barone, V.; Petersson, G. A.; Nakatsuji, H.; Li, X.; Caricato, M.; Marenich, A. V.; Bloino, J.; Janesko, B. G.; Gomperts, R.; Mennucci, B.; Hratchian, H. P.; Ortiz, J. V.; Izmaylov, A. F.; Sonnenberg, J. L.; Williams-Young, D.; Ding, F.; Lipparini, F.; Egidi, F.; Goings, J.; Peng, B.; Petrone, A.; Henderson, T.; Ranasinghe, D.; Zakrzewski, V. G.; Gao, J.; Rega, N.; Zheng, G.; Liang, W.; Hada, M.; Ehara, M.; Toyota, K.; Fukuda, R.; Hasegawa, J.; Ishida, M.; Nakajima, T.; Honda, Y.; Kitao, O.; Nakai, H.; Vreven, T.; Throssell, K.; Montgomery, J. A., Jr.; Peralta, J. E.; Ogliaro, F.; Bearpark, M. J.; Heyd, J. J.; Brothers, E. N.; Kudin, K. N.; Staroverov, V. N.; Keith, T. A.; Kobayashi, R.; Normand, J.; Raghavachari, K.; Rendell, A. P.; Burant, J. C.; Iyengar, S. S.; Tomasi, J.; Cossi, M.; Millam, J. M.; Klene, M.; Adamo, C.; Cammi, R.; Ochterski, J. W.; Martin, R. L.; Morokuma, K.; Farkas, O.; Foresman, J. B.; Fox, D. J. *Gaussian 16*, Revision A.03; Gaussian, Inc.: Wallingford, CT, 2016.
(51) Becke, A. D. Density-functional thermochemistry. III. The role of exact Exchange. *J. Chem. Phys.* **1993**, *98*, 5648−5652.
(52) Dunning, T. H., Jr Gaussian basis sets for use in correlated molecular calculations. I. The atoms boron through neon and hydrogen. *J. Chem. Phys.* **1989**, *90*, 1007−1023.
(53) Tomasi, J.; Mennucci, B.; Cammi, R. Quantum mechanical continuum solvation models. *Chem. Rev.* **2005**, *105*, 2999−3093.
(54) Grimme, S.; Antony, J.; Ehrlich, S.; Krieg, H. A. Consistent and accurate *ab initio* parametrization of density functional dispersion correction (DFT-D) for the 94 elements H-Pu. *J. Chem. Phys.* **2010**, *132*, 154104−154119.

https://doi.org/10.1021/acscatal.5c01335
ACS Catal. 2025, 15, 9117−9129

(55) *AIMAll*, Version 19.10.12; Developed by Todd A. Keith; TK Gristmill Software: Overland Park, KS, 2019.
(56) Espinosa, E.; Molins, E.; Lecomte, C. Hydrogen bond strengths revealed by topological analyses of experimentally observed electron densities. *Chem. Phys. Lett.* **1998**, *285*, 170−173.
(57) Wolinski, K.; Hinton, J. F.; Pulay, P. Efficient Implementation of the Gauge-Independent Atomic Orbital Method for NMR Chemical Shift Calculations. *J. Am. Chem. Soc.* **1990**, *112*, 8251−8260.

https://doi.org/10.1021/acscatal.5c01335
ACS Catal. 2025, 15, 9117−9129